Interannual and Decadal Variability of the North Pacific Blocking and Its Relationship to SST, Teleconnection and Storm Tracks

Huang Fei (黄 非)[1], Zhou Faxiu (周发琇) and Qian Xiaodan (钱筱丹)

Department of Marine Meteorology, Ocean University of Qingdao, Qingdao 266003

(Received August 22, 2001; revised May 10, 2002)

ABSTRACT

Climatological features of mid-latitude blocking occurring over the North Pacific Ocean during 52 winters (December to February) of 1948/1949–1999/2000 are statistically analyzed based on NCEP/NCAR reanalysis data. Significant interannual variation with a period of about 3–7 years as well as decadal variability is found by wavelet analysis and power spectrum analysis. A decreasing trend of the 2–7 year bandscale-averaged variance occurs throughout the 52 years and an abrupt shift from a higher state to a lower state during the 1970s is also found, which suggests an interdecadal variation of the North Pacific blocking. The possible relationship between the variability of blocking and sea surface temperature (SST), storm tracks and teleconnection are shown using composite analysis. In strong blocking anomaly winter (SBW), the geopotential height anomaly at 500 hPa exhibits a typical PNA (Pacific-North American)-like wave-train pattern in the North Pacific. The storm tracks, representing the activity of transient eddies, extend northeastward to the western coast of North America along the mid latitudes of about 40°–50°N, with the SST anomaly exhibiting a Pacific decadal oscillation (PDO) mode at mid-latitude and a La Niña-like pattern along the equator. Contrasting features appear in weak blocking anomaly winter (WBW).

Key words: north Pacific blocking, teleconnection, SST anomaly, and storm tracks

1. Introduction

Blocking is a large-scale, mid-latitude atmospheric phenomenon that has a profound effect on local and regional climates in the immediate blocking domain (Rex 1950a, b; Illari 1984) as well as in regions upstream and/or downstream of the blocking event (Quiroz 1984; White and Clark 1975). Therefore, it has long been a primary interest of many synoptic and dynamical meteorologists for decades.

Many studies have derived a comprehensive set of climatological statistical characteristics of blocking anticyclones using subjective or objective techniques, including location, frequency, duration, intensity, size, seasonal and regional distribution (Elliott and Smith 1949; Rex 1950a, b; White and Clark 1975; Lupo and Smith 1995; Lejenäs and Økland 1983). These have shown that the Pacific region is accepted to be one of the two preferred regions for the occurrence of blocking in the Northern Hemisphere.

[1]E-mail: huangf@mail.ouqd.edu.cn

In their pioneering studies, there are three categories of methods to identify blocking events. The first is a subjective technique, put forward earliest by Rex in the 1950s (Rex 1950a, b) and was inherited and modified by Sumner (1954) and White and Clark (1975). They identified the blocking events subjectively by visual inspection and then used semi–objective criteria to determine the exact dates of initiation and duration of blocking based on examining the daily weather charts. The second is an objective criteria first used by Elliott and Smith (1949) based on magnitude and persistence of pressure departure from normal. Then Hartmann and Ghan (1980), Dole (1982), Shukla and Mo (1983), and Zhao and Chen (1990) extended it from sea level pressure departure to upper level geopotential height departure from normal. The last objective criteria to identify blocking events was designed by Lejenäs and Økland (1983). They used the north–south geopotential height gradient based on the coherence between the mid–latitude low westerly index and blocking. The advantage of this objective method is its simplicity for automatic calculation on computer and was therefore widely used by Tibaldi and Molteni (1990) and D'Andrea et al. (1998) with a certain amount of modification.

It is interesting to note that the papers by Elliott and Smith (1949) and Rex (1950b), which were published within a year of each other, gave contradictory results on the relative frequency of blocking in the Atlantic and Pacific. White and Clark (1975) also obtained results that were not in agreement with Rex (1950b). It should be remarked that these differences between authors are mainly due to the use of different data in different time periods, as well as different criteria to identify blocking events. It is possible that the above differences reflect the interannual or decadal variability of blocking actions. Few studies focusing on this aspect of blocking have been published until now, although the important role of high–frequency waves on blocking formation and maintenance has been confirmed (Berggren et al. 1949; Rex 1950a, b; Green 1977; Holopainen and Fortelius 1987; Nakamura et al. 1997; Luo 1999, 2000a, b; Luo and Li 2000). In addition, the climatological variability of transient eddies or "storm tracks" relative to blocking is still not so clear. Therefore, it is important to understand whether there exists interannual or decadal variability for Pacific blocking actions. Since blocking is a mid–latitude atmospheric phenomenon and its variation reflects the anomaly of the general circulation in mid–latitude, it may be strongly affected by tropical Pacific SST fluctuations associated with El Niño–Southern Oscillation (ENSO) episodes, and may also respond to the less robust signal associated with mid–latitude SST anomalies (Lau 1997). If so, whether it is related to ENSO, which is regarded as the strongest signal of interannual variation of climate, or whether it possesses some relationship with Pacific Decadal Oscillation (PDO), the most significant mode for mid–latitude Pacific ocean, this paper attempts to examine the possible relationships between them.

The paper is organized as follows. In section 2, the data set and the method used are described. Section 3 is devoted to examine the interannual and decadal variability of the North Pacific blocks throughout 52 winters. In section 4, we focus on the composite features of anomalous 500 hPa geopotential height, sea surface temperature anomaly, and storm track activity. Concluding remarks are found in section 5.

2. Data and methodology

The primary database for this study consists of daily 500 hPa geopotential height (HGT) grid point reanalysis data on a 2.5° latitude × 2.5° longitude grid provided by NCEP/NCAR. The data domain extends from 0° to 90°N, and the period of coverage extends from 1

January 1948 through 31 December 2000. The winter season is taken to be the 3–month mean from December to February. The other data used in this study comes from version #7 of a retrospective analysis of the global ocean based on the Simple Ocean Data Assimilation (SODA) package of Carton et al. (2000a, b). The analysis is monthly and spans the period of January/ 1950–December/ 1999, with a resolution of about 1° longitude $\times$ 1° latitude. The most upper level (7.5 m) sea temperature is regarded as the sea surface temperature (SST).

In order to accentuate the synoptic scale disturbances with characteristic periods of several days, the "bandpass" filter described in Trenberth (1986), which retains fluctuations with 2.5–6 day periods, has been applied to the daily time series of the geopotential height. The filtered time series for 500 hPa height were then partitioned into individual monthly segments, one for every winter month. For each monthly segment, the temporal root–mean–square (rms) values were then computed for that segment. Hence, one obtains 52 data fields altogether, with each field corresponding to the bandpass–filtered rms pattern of 500 hPa height for a certain winter season. In conformity with terminology adopted in a majority of published works on this subject, we shall continue to refer to the elongated maxima in the rms of bandpass (2.5–6 day) filtered geopotential height as the " storm tracks", with the understanding that these storm tracks portray preferred migration paths of both positive and negative synoptic–scale perturbations.

Throughout this study, removal of the climatologically seasonal cycle from the monthly mean fields has been accomplished by subtracting the long–term averaged values for a given calendar month from corresponding values of the same month in individual years.

Wavelet analysis is becoming a common tool for analyzing localized variations of power within a time series. By decomposing a time series into time–frequency space, one is able to determine both the dominant modes of variability and how those modes vary in time. Therefore, in order to identify the detailed characteristics of the Pacific blocking time series in the time and frequency domain, wavelet analysis with a wavelet basis function named "Morlet" is used. Readers who are interested in this method can refer to the article by Torrence and Compo (1998).

3. Interannual and decadal variability for blocking actions

Following the second approach of adopting objective criteria as suggested by Dole (1982), all North Pacific blocking cases occurring in the winter season were identified from 1948 to 2000. In order to depict the variation of blocking, four indexes were defined as follows. The first index is called the frequency index (FI), which is defined as the total number of days in which blocking occurred each winter. This time series shows how often the North Pacific blocking occurs. The second is named the area index (AI), defined as the winter–averaged total number of grid points that the 500 hPa height anomaly greater than 100 gpm covered over the North Pacific (Dole and Gordon 1983) in which the blocking prefers to occur. This index indicates the extent of the blocking and is defined in a similar manner to the area index for the subtropical high. The degree of blocking intensity (DI) is the third index, defined as the averaged difference between the 500 hPa geopotential height anomaly at each grid point where blocking occurs minus 100. The last index is defined as PI = DI / AI, also showing the intensity of the blocking. All four indexes can indicate the North Pacific blocking variations from different points of view such as its frequency, extent, and intensity.

Figure 1 shows the time series of the four indexes for blocking during 1948–2000. It is obvious that the occurrence of the North Pacific blocking in winter has an apparent interannual variation, not only the frequency of blocking occurrence, but also the extent and intensity. The correlation coefficients between the four indexes are all larger than 0.92 suggesting the coherence of the blocking's frequency, range, and intensity during the 52 winters, which agrees with many previous results (Hartman and Ghan 1980; Lejenäs and Økland 1983; Lupo and Smith 1995). The variations of the North Pacific blocking fluctuate up and down with several–year oscillations. It is remarkable that a sharp weakening occurred in the mid–1970s and a relative strengthening of blocking appeared before the 1970s, therefore giving a decreasing tendency throughout the 52 winters. This feature can be seen more clearly from the shaded lines smoothed with a 7–point running mean in Fig. 1, highlighting the decadal variation and decreasing trend.

Discrete power spectrum analysis shows that the dominant period of oscillation for these time series is about 4–7 years (figure omitted). The same result and more detailed information

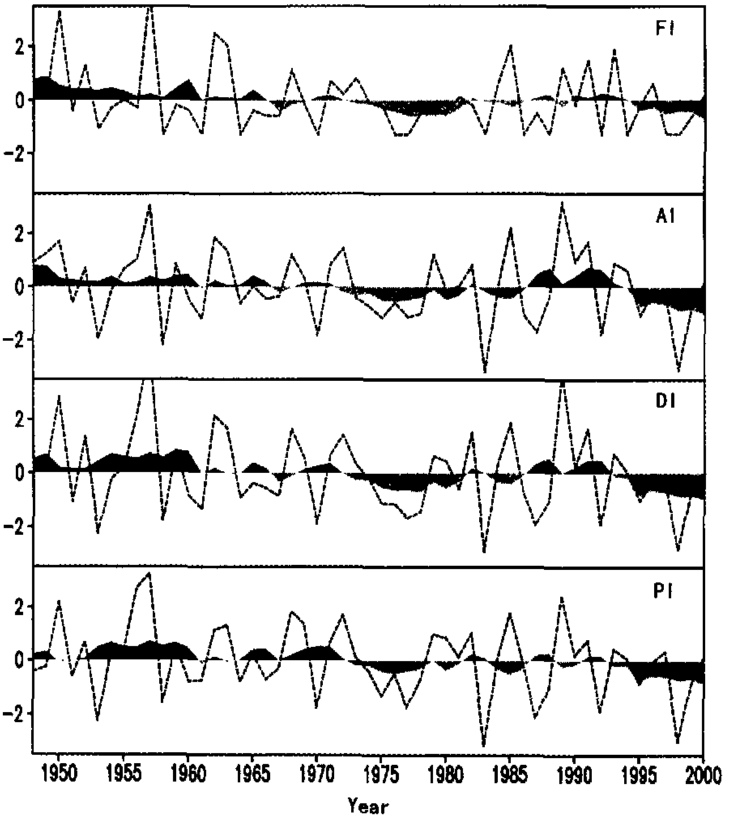

Fig. 1. Time series of the four indexes for blocking over the North Pacific during the winters from 1948 / 1949 to 1999 / 2000. Shown, from top to bottom, are the FI, AI, DI, and PI standardized indexes, respectively. The shaded lines in each panel have been smoothed with a 7–point running mean.

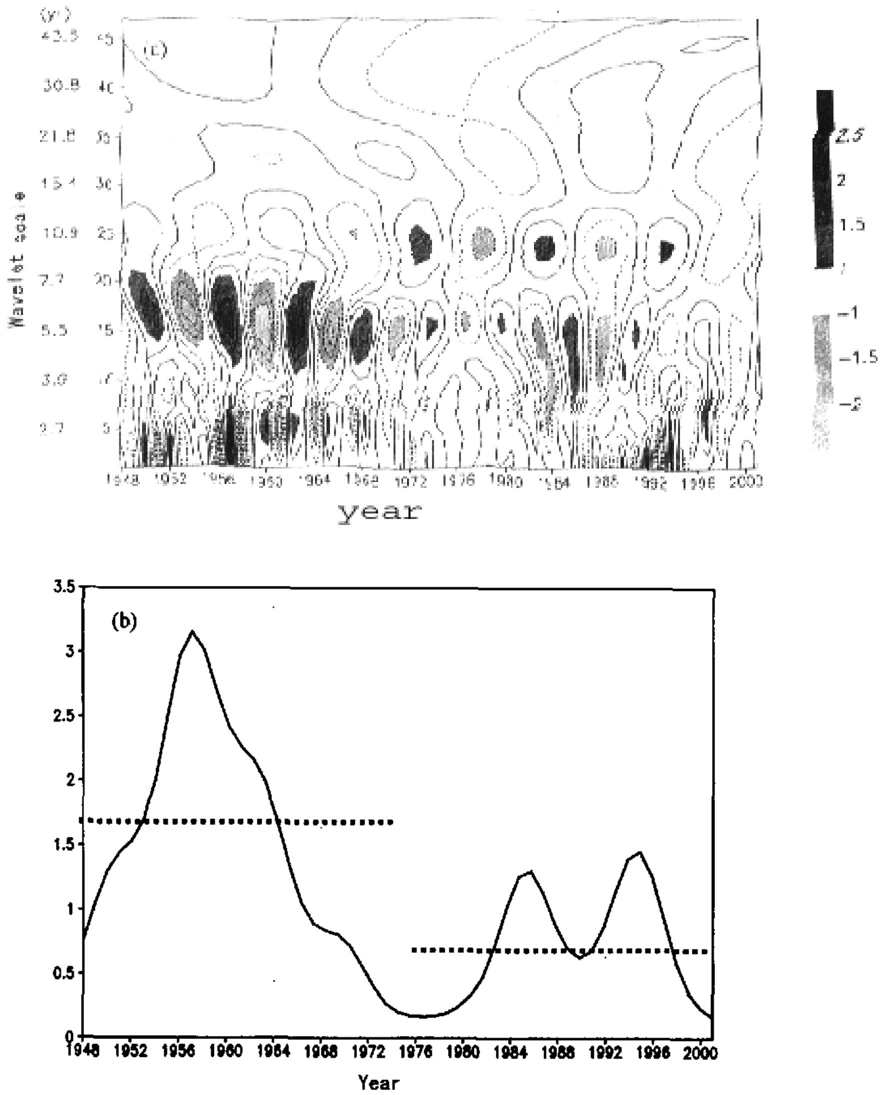

Fig. 2. (a) Real part distribution of the wavelet transform coefficient for FI index by using the Morlet wavelet basis function in the time and frequency domain. The abscissa is time (year) and the ordinate is wavelet scale. The corresponding period (year) to the scale is shown in the left ordinate. The contour interval is 0.5 and solid lines mean positive values while dashed lines mean negative values. The dark and light shaded regions represent areas >1 and <−1, respectively. (b) Scale−averaged wavelet variance spectrum over the 2−7 year bands for the time series of FI index. The dashed lines are the mean values of the two different states.

are also obtained by wavelet analysis. Figure 2a shows the real–part distribution of the wavelet transform coefficient for the time series of FI in both the time and frequency domain. The most impressive feature is that most of the amplitude contribution is concentrated within the band of 4–7 year although there is appreciable values at shorter periods. It is also shown that a period with quasi–10 years becomes significant after the 1970s. An interesting characteristic is that there exists a sudden split in frequency from middle frequency (with a period of 4–7 year) to a lower frequency (with a period of quasi–10 year) and a slightly higher frequency (with a period of 3–5 year) during the 1970s. To examine the fluctuations in variance over interannual time scales (the band of 2–7 year), the scale–averaged wavelet energetic power, which is a time series of the averaged variance in a certain band, is shown in Fig. 2b. The solid line shows the average variance over the 2–7 year bands versus time, which appears as a consistent decreasing trend and an abrupt shift from a higher state to a lower state during the 1970s. This may suggest the amplitude variation of the blocking's interannual vibration modulates on longer time scales of variation, referring to the decadal and interdecadal variability for blocking.

4. Composite fields related to blocking variation

Based on the variability of the four indexes for the North Pacific blocking in Fig. 1, ten winters with high blocking indexes (four standardized indexes all greater than 0.5) and eleven winters with low blocking indexes (four standardized indexes all less than –0.5) are chosen for composite analysis. The blocking often occurs with strong intensity during high–indexes winters and so these winters are called strong blocking winters (SBW), and similarly, low–indexes winters are called weak blocking winters (WBW). There are 10 years of SBW, including 1949/50, 1951/52, 1956/57, 1961/62, 1962/63, 1967/68, 1970/71, 1984/85, 1988/89, and 1990/91; and 11 years of WBW, consisting of 1952/53, 1957/58, 1960/61, 1963/64, 1969/70, 1976/77, 1982/83, 1986/87, 1991/92, 1997/98, and 1998/99. It is noticeable there are nine years of WBW relevant to the El Niño years, while half of SBW correspond to the La Niña years according to Angell (1981) and Rasmusson and Carpenter (1982). The following results are based on the 10–year or 11–year composites in SBW or WBW, respectively.

4.1 *Sea surface temperature (SST)*

In order to find the relationship between the North Pacific blocking and the sea surface temperature, SST anomaly composite fields in SBW and WBW are drawn in Figure 3a and b, respectively. The most prominent feature in the SST anomaly composite field in SBW is the large areas of negative SST anomaly in the central to eastern tropical Pacific, offshore of the western coast of North America and the western part of the subtropical gyre south of the Kuroshio extension, while the positive SST anomaly covers the western tropical Pacific, the so–called warm pool, and mid–latitudes in the North Pacific. During the opposite period in WBW the composite SST anomaly field has almost the contrary pattern compared with SBW. The most striking distinction between the two composites is the difference of the leading significant areas that are shaded in Fig. 3. In SBW, the most significant SST anomaly is located in the central Pacific at mid–latitude with a maximum positive value greater than 0.8°C, whereas in WBW the most significant SST anomaly is located along the central to eastern equator with a maximum positive value greater than 1.4°C, which is a typical El Niño pattern. These results suggest that North Pacific mid–latitude atmospheric blocking is not only related

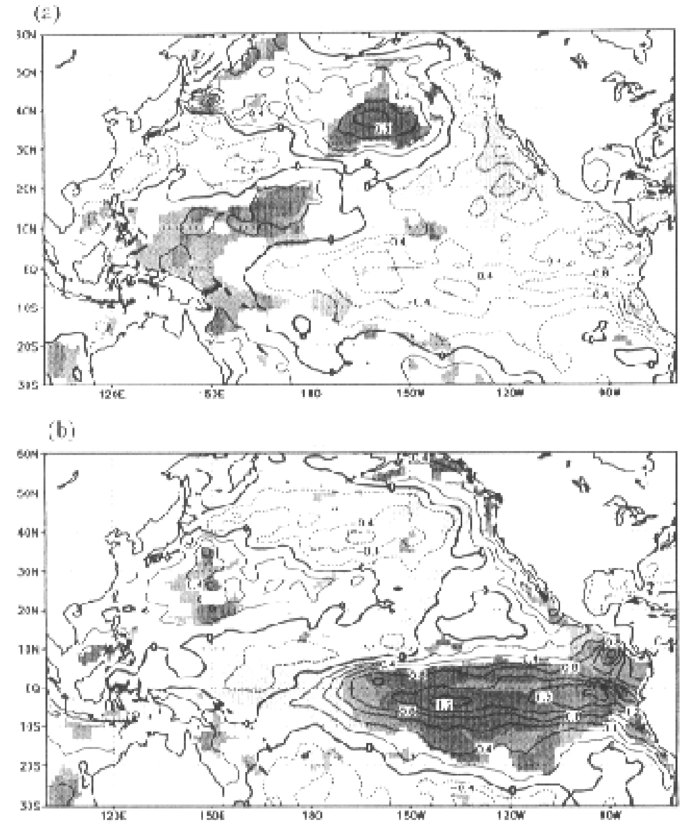

Fig. 3. Composite fields of SST anomaly in (a) SBW and (b) WBW. The contour interval is 0.2°C. Thin solid lines are values greater than zero, dashed lines are values less than zero, and thick solid lines are the zero line. The grey shaded areas correspond to areas exceeding the 95% confidence level by the student *t*–test.

to the local SST anomaly, but also has a connection with the SST anomaly in the equatorial Pacific. The later corresponds to the well–known interannual ENSO phenomenon, which may indirectly impact the mid–latitude atmospheric blocking through teleconnection, mainly contributing to the interannual timescale variability of the North Pacific blocking. Note that the former SST anomaly pattern is similar to the PDO mode (Latif and Barnett 1994; Zhang et al. 1997), which may contribute to the interdecadal variation of the North Pacific blocking.

4.2 *The 500 hPa geopotential height*

In order to reveal the connection between the blocking variability and atmospheric teleconnection, composite fields of the 500 hPa geopotential height anomaly during SBW and WBW were drawn in Fig. 4a and Fig. 4b, respectively. The remarkable pattern is a typical PNA (Pacific / North America)–like wave train (Wallace and Gutzler 1981) from the western and central Pacific to the eastern Pacific along a Rossby big circle trace (the thick dashed

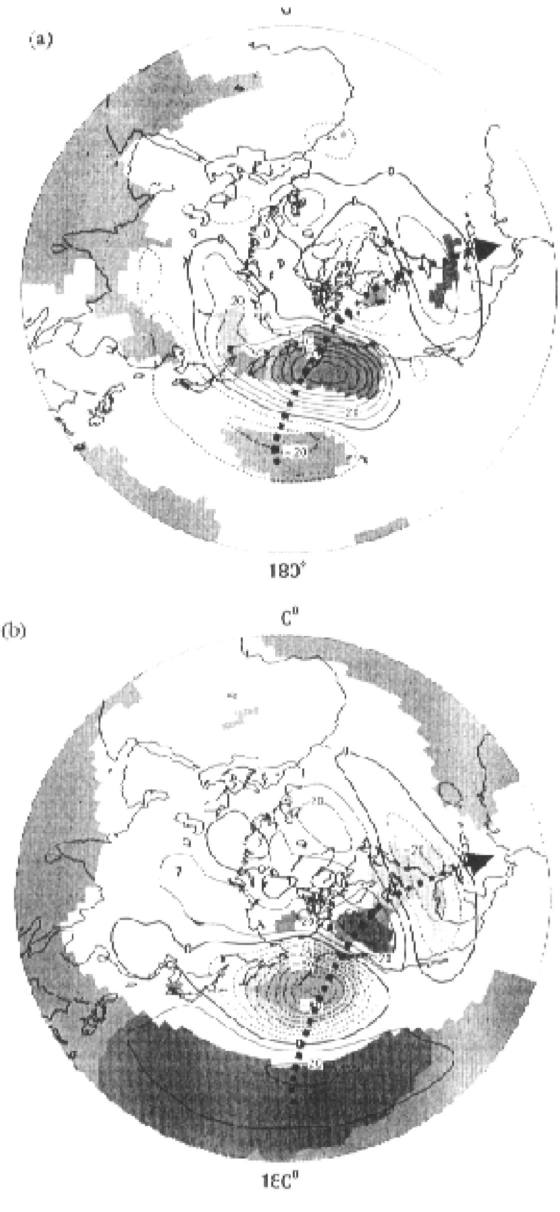

Fig. 4. Composite fields of the 500 hPa geopotential height anomaly in (a) SBW and (b) WBW. Contour interval is 10 gpm. Solid lines are the values greater than zero, dashed lines are values less than zero, and thick solid lines are the zero line. The grey shaded areas correspond to areas exceeding the 95% confidence level by the student t-test. The thick dashed arrow gives the direction of wave train.

curve with arrow). The negative and positive centers of the geopotential height anomaly queued up forming a '−' '+' '−' '+' wave train directed from the subtropical central Pacific northeastward to North America. The wave trains in SBW and WBW take on almost completely reversed signs. The maximum positive anomalous center is located near the Aleutian archipelagos in SBW, which just corresponds to the preferred position of the North Pacific blocking high, while the minimum negative anomalous center in the wave train is found at the position in WBW, representing the strengthening of the Aleutian Low. This pattern means that in SBW, the North Pacific blocks occur frequently and correspond to the 500 hPa height anomaly with a positive PNA teleconnection pattern that connects the mid−latitude blocking to the tropics. While in WBW, few blocks occur corresponding to a negative PNA teleconrection at 500 hPa pressure level. Some studies (Horel and Karoly 1981; Rasmusson and Carpenter 1982; Lau 1997) have pointed out that these kind of atmospheric patterns were significantly correlated with ENSO−related SST changes in the tropical Pacific. Therefore, considering the relationship between the mid−latitude blocking and the Pacific SST anomaly discussed in section 4.1, this PNA−like teleconnection pattern may be the atmospheric bridge that connects the interaction between the anomalous circulation related to the blocking at mid−latitudes and the variation of the tropical SST on the interannual time scale.

It is noticeable that the significant difference between the composite fields in SBW and WBW, except for the opposite sign of wave trains, lies in the shaded areas illustrating the significance of differences at the 95% confidence level by a student t−test. In SBW, the regions exceeding the 95% confidence level are mainly distributed along the wave train with separated centers, which seems to emphasis the local effect for the mid−latitude air−sea interaction related to the PDO mode for SST anomaly (Latif and Barnett 1994; Zhang et al. 1997). And this may be linked to the decadal variability of the North Pacific blocking. However, in WBW, the areas exceeding the 95% confidence level are not only distributed along the centers of the wave train, but almost cover all the tropical oceans. The wave train starts off from the central tropical Pacific and then extends northeastward, suggesting the possible linkage between the interannual variability of the mid−latitude blocking and the tropical SST anomaly, or ENSO mode.

4.3 *Variability of atmospheric storm tracks*

Previous studies have shown that the Pacific SST anomaly during boreal winter can affect the axis of the storm track over the Pacific (Held et al. 1989; Hoerling and Ting 1994; Straus and Shukla 1997). The relation between the storm track and blocking over the North Pacific has yet to be studied. Composite fields of rms of bandpass−filtered (2.5−6 day) 500 hPa geopotential height in SBW and WBW, are shown in Fig. 5a and Fig. 5b, respectively. In WBW the storm track is most intense along 40°N with a maximum center around the dateline. In SBW, however, the storm track extends northeastward and the rms maximum center is split into two centers, one is still along 40°N spanning from 160°E−180° and the other moves to about 50°N reaching to the west coast of North America. The difference in rms of bandpass−filtered 500 hPa geopotential height (Fig. 5c) between that in SBW and that in WBW is shown superimposed on the significance of differences at the 95% level. A PNA−like pattern is apparent in Fig. 5c, extending northeastward to North America from the tropical Pacific. As many studies have shown manifested (e.g., Webster 1981, 1982; Palmer and Sun 1985; Lau and Nath 1990; Ferranti et al. 1994), anomalous SST will result in anomalous transient eddy activity in the atmosphere by baroclinic instability. Linking with Fig. 3a, the positive mid−latitude SST anomaly would weaken the meridional SST gradient at

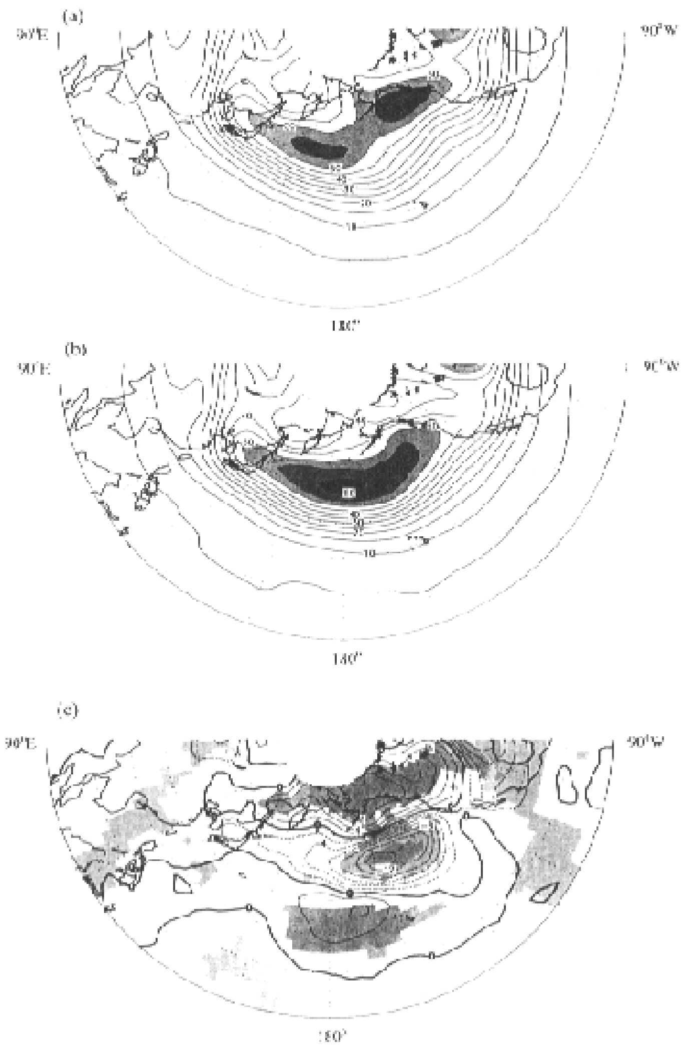

Fig. 5. Composite fields of rms of bandpass-filtered 500 hPa geopotential height in (a) SBW and (b) WBW. Contour interval is 5 gpm. (c) Difference field between (a) and (b). Solid lines are values greater than zero, dashed lines are values less than zero, and thick solid lines are the zero line. The grey shaded areas correspond to areas exceeding the 95% confidence level by the student t-test.

the mid-latitude ocean and result in a northward shift of the baroclinic eddy activity in the atmosphere (Palmer and Sun 1985; Lau and Nath 1990; Ferranti et al. 1994), leading to reduced westerly winds over mid-latitude ocean, accompanied by anomalous high pressure (blocking high) over the North Pacific (Shutts 1983; Luo 2000a; Luo et al. 2001). Therefore, the variability of the North Pacific blocking may be linked with SST anomaly in two ways:

the first direct way is the mid–latitude local SST anomaly affecting the storm track through air–sea interaction as well as impacting the variability of blocking; the other way is indirect, where the mid–latitude atmospheric blocking responds to the tropical SST anomaly by teleconnection.

5. Conclusions and discussions

The interannual and decadal characteristics of the North Pacific blocking during the Northern winters from 1948 / 1949–1999 / 2000 are examined. The frequency, range, and intensity of blocking over the North Pacific all have significant interannual variations with period of about 3–7 year as well as decadal variability confirmed by wavelet analysis and power spectrum analysis. A decreasing trend of the 2–7 year bandscale–averaged variance occurred throughout the 52 years and an abrupt shift from a higher state to a lower state during the 1970s is found. This may suggest the amplitude variation of the blocking's interannual vibration modulates on longer time scales of variation, referring to the decadal and interdecadal variability for blocking.

Composite analysis shows that in SBW the geopotential height anomaly at 500 hPa exhibits a typical PNA–like wave–train pattern in the North Pacific (Wallace and Gutzler 1981). And the storm tracks, representing the activity of transient eddies, extend northeastward to the western coast of North America along the mid latitudes of about 40°–50°N, with the SST anomaly appearing in a PDO mode in mid–latitudes and in a La Niña–like pattern along the equator. On the other hand, a negative PNA–like pattern (Wallace and Gutzler 1981) for the 500 hPa geopotential height anomaly, a zonal storm track around the dateline with one center along 40°N, and a typical El Niño–like pattern in the Pacific SST anomaly are obtained during WBW. These results indicate a possible relationship between the North Pacific blocking action, storm tracks and the SST anomaly, which will be helpful for revealing the possible mechanism of interannual and decadal variability of blocking. The possible mechanism may be described like this: the mid latitude PDO–like SST anomaly pattern would weaken the meridional SST gradient at the mid–latitude ocean and result in a northward shift of the baroclinic eddy activity in the atmosphere (Palmer and Sun 1985; Lau and Nath 1990; Ferranti et al. 1994), leading to reduced westerly winds over mid–latitude ocean, accompanied by anomalous high pressure (blocking high) over the North Pacific (Shutts 1983; Luo 2000a; Luo et al. 2001). This is a direct response in the atmosphere to mid–latitude SST anomaly, giving rise to the decadal variation of blocking modulated on an interannual oscillation. Furthermore, there still exists an indirect response to the tropical ENSO–like SST anomaly, the so–called teleconnection, which may mainly determine the interannual variability of blocking. This paper just provides the possible relation between the Pacific blocking, storm tracks and the SST anomaly with teleconnection by composite analysis; the relationship between them on different timescales has yet to be studied.

Acknowledgments. The authors would like to thank two anonymous reviewers for their useful suggestions on the original manuscript of this paper. The authors would also like to thank the atmospheric data center of the Nanjing Meteorological Institute for supplying the NCEP / NCAR reanalysis data and Professor Ruixin Huang of the Woods Hole Oceanography Institute for supplying the SODA data.

REFERENCES

Angell, J. K., 1981: Comparison of variations in atmospheric quantities with sea surface temperature variation in the equatorial eastern Pacific. *Mon. Wea. Rev.*, **109**, 230–243.

Berggren, R., B. Bolin, and C. G. Rossby, 1949: An aerological study of zonal motion, its perturbations and break-down. *Tellus*, **2**, 14–37.

Carton, J. A., G. Chepurin, X. Cao, and B. S. Giese, 2000a: A simple ocean data assimilation analysis of the global upper ocean 1950–1995. Part 1: Methodology. *J. Phys. Oceanogr.*, **30**, 294–309.

Carton, J. A., G. Chepurin, and X. Cao, 2000b: A simple ocean data assimilation analysis of the global upper ocean 1950–1995. Part 2: Results. *J. Phys. Oceanogr.*, **30**, 311–326.

D'Andrea, F. S. Tibaldi and M. Blackburn et al., 1998: Northern Hemisphere atmospheric blocking as simulated by 15 atmospheric general circulation models in the period 1979–1988. *Climate Dynamics*, **14**, 385–407.

Dole, R. M., 1982: Persistent anomalies of the extratropical Northern Hemisphere wintertime circulation. Ph.D. dissertation. Massachusettes Institute of Technology, 225pp.

Dole, R. M., and N. D. Gordon, 1983: Persistent anomalies of the extra–tropical Northern Hemisphere wintertime circulation: Geographical distribution and regional persistence characteristics. *Mon. Wea. Rev.*, **111**, 1567–1586.

Elliott, R. D., and T. B. Smith, 1949: A study of the effects of large blocking highs on the general circulation in the Northern Hemisphere westerlies. *J. Meteor.*, **6**, 27–85.

Ferranti, L., F. Molteni, and T. N. Palmer, 1994: Impact of localized tropical and extratropical SST anomalies in ensembles of seasonal GCM integrations. *Quart. J. Roy. Meteor. Soc.*, **120**, 1613–1645.

Green, J. S. A., 1977: The weather during July 1976: Some dynamical considerations of the drought. *Weather*, **32**, 120–128.

Hartman, D. L., and S. J. Ghan, 1980: A statistical study of the dynamics of blocking. *Mon. Wea. Rev.*, **108**, 1144–1159.

Held, I. M., S. W. Lyons, and S. Nigam, 1989: Transients and extratropical response to El Niño. *J. Atmos. Sci.*, **46**, 163–174.

Hoerling, M. P., and M. Ting, 1994: Organization of extratropical transients during El Niño. *J. Climate*, **7**, 745–766.

Holopainen, E., and C. Fortelius, 1987: High–frequency transient eddies and blocking. *J. Atmos. Sci.*, **44**, 1632–1645.

Horel, J. D., and D. J. Karoly, 1981: Planetary scale atmospheric phenomena associated with the Southern Oscillation. *Mon. Wea. Rev.*, **109**, 813–829.

Illari, L., 1984: A diagnostic study of the potential vorticity in a warm blocking anticyclone. *J. Atmos. Sci.*, **41**, 3518–3526.

Latif, M., and T. P. Barnett, 1994: Causes of decadal climate variability over the North Pacific and North America. *Science*, **266**, 634–637.

Lau, N.–C., and M. J. Nath, 1990: A general circulation model study of the atmospheric response to extratropical SST anomalies observed in 1950–1979. *J. Climate*, **3**, 965–989.

Lau, N–C, 1997: Interactions between global SST anomalies and the midlatitude atmospheric circulation. *Bull. Amer. Meteor. Soc.*, **78**, 21–33.

Lejenäs, H., and H. Økland, 1983: Characteristics of Northern Hemisphere blocking as determined from a long time series of observational data. *Tellus*, **35A**, 350–362.

Luo, D., 1999: *Large–Scale Envelope Rossby Solitons in the Atmosphere and Blocking Circulations*. China Meteorological Press, Beijing, 113pp (in Chinese).

Luo, D., 2000a: Planetary–scale baroclinic envelope Rossby solitons in a two–layer model and their interaction with synoptic–scale eddies. *Dynamics of Atmospheres and Oceans*, **32**, 27–74.

Luo, D., 2000b: *Nonlinear Dynamics of Blocking*. China Meteorological Press, Beijing, 248pp (in Chinese).

Luo, D., and J. Li, 2000: Barotropic interaction between planetary–and synoptic–scale waves during the life cycle of blocking. *Advances in Atmospheric Sciences*, **17**, 649–670.

Luo, D., F. Huang, and Y. Diao, 2001: Interaction between antecedent planetary–scale envelope soliton blocking anticyclone and synoptic–scale eddies: Observations and theory. *J. Geophys. Res.*, **106**(D23), 31, 795–31, 815.

Lupo, A. R., and P. J. Smith, 1995: Climatological features of blocking anticyclones in the Northern Hemisphere. *Tellus*, **47a**, 439–456.

Nakamura, H., M. Nakamura, and J. L. Anderson, 1997: The role of high– and low–frequency dynamics in blocking formation. *Mon. Wea. Rev.*, **125**, 2074–2093.

Palmer, T. N., and Z. Sun, 1985: A modeling and observational study of the relationship between sea surface temperature in the north–west Atlantic and the atmospheric general circulation. *Quart. J. Roy. Meteor. Soc.*, **111**, 947–975.

Quiroz, R. S., 1984: The climate of the 1983–84 winter: A season of strong blocking and severe cold in North America. *Mon. Wea. Rev.*, **112**, 1894–1912.

Rasmusson, E. M., and T. H. Carpenter, 1982: Variations in tropical sea surface temperature and surface wind fields associated with the Southern Oscillation / El Niño. *Mon. Wea. Rev.*, **110**, 354–384.

Rex, D. F., 1950a: Blocking action in the middle troposphere and its effects upon regional climate. I. An aerological study of blocking action. *Tellus*, **2**, 196–211.

Rex, D. F., 1950b: Blocking action in the middle troposphere and its effects upon regional climate. II. The climatology of blocking action. *Tellus*, **2**, 275–301.

Shukla, J., and K. C. Mo, 1983: Seasonal and geographical variation of blocking. *Mon. Wea. Rev.*, **111**, 388–402.

Shutts, G. J., 1983: The propagation of eddies in diffluent jetstreams: Eddy vorticity forcing of blocking flow fields. *Quart. J. Roy. Meteor. Soc.*, **109**, 737–761.

Straus, D. M., and J. Shukla, 1997: Variations of midlatitude transient dynamics associated with ENSO, *J. Atmos. Sci.*, **54**, 777–790.

Sumner, E. J., 1954: A study of blocking in the Atlantic–European sector of the Nothern Hemisphere. *Quart. J. R. Meteor. Soc.*, **80**, 802–816.

Tibaldi, S., and F. Molteni, 1990: On the operational predictability of blocking. *Tellus*, **42A**, 343–365.

Torrence, C., and G. P. Compo, 1998: A practical guide to wavelet analysis. *Bull. Amer. Meteor. Soc.*, **79**, 61–78.

Trenberth, K. E., 1986: An assessment of the impact of transient eddies on the zonal flow during a blocking episode using localized Eliassen–Palm flux diagnostics. *J. Atmos. Sci.*, **43**(10), 2070–2087.

Wallace, J. M., and D. S. Gutzler, 1981: Teleconnections in the geopotential height field during the Northern Hemisphere winter. *Mon. Wea. Rev.*, **109**, 784–812.

Webster, P. J., 1981: Mechanisms determining the atmospheric response to sea surface temperature anomalies. *J. Atmos. Sci.*, **38**, 554–571.

Webster, P. J., 1982: Seasonality in the local and remote atmospheric response to sea surface temperature anomalies. *J. Atmos. Sci.*, **39**, 41–52.

White, E. B., and N. E. Clark, 1975: On the development of blocking ridge activity over the central North Pacific. *J. Atmos. Sci.*, **32**, 489–501.

Zhang, Y., J. M. Wallace, and D. S. Battisti, 1997: ENSO–like interdecadal variability: 1900–1993. *J. Climate*, **10**, 1004–1020.

Zhao Hanguang, and Chen Xuezhen, 1990: Statistical analysis for Northern Hemispheric blocking high. *Meteorology*, **16**(3), 3–7 (in Chinese).

北太平洋阻塞的年际年代际变化及其与SST、遥相关及风暴路径的关系

黄 非 周发琇 钱筱丹

摘 要

利用 NCEP/NCAR 再分析资料，对 1948/1949–1999/2000 共 52 个冬季的北太平洋上空中纬度阻塞异常的气候特征进行了统计分析，小波分析和功率谱分析结果表明该区域阻塞发生的频数具有很明显的 3–7 年的年际振荡和年代际变化特征。同时 2–7 年带通平均的小波方差谱分析结果表明阻塞的这种年际变化的振幅存在着缓慢下降的趋势，且气候突变在 20 世纪 70 年代，这进一步证明了北太平洋上空的阻塞活动具有年代际变化特征。对强阻塞异常的冬季和弱阻塞异常的冬季分别进行合成分析，结果表明，对于阻塞异常强的冬季，北太平洋 500 hPa 高度异常场表现为典型的 PNA 型的波列，风暴路径则在 40°–50°N 之间从日界线以西向东北方向加强并分裂成两个中心，而 SST 异常在中纬度太平洋则对应着典型的 PDO 型，在赤道地区则为类 La Niña 型的海温分布。而对于阻塞异常弱的冬季则对应截然不同甚至相反的分布特征，即 500 hPa 高度异常场表现为符号相反的 PNA 型，风暴路径中心在日界线附近呈纬向型分布，同时 SST 异常在赤道地区则为典型的 El Niño 型的海温分布。以上结果揭示出北太平洋阻塞活动的年际变化可能主要与热带海温的遥响应相联系，而年代际变化则主要与中纬度局地的 PDO 型海温及其通过斜压瞬变波的海–气相互作用有关。

关键词：北太平洋阻塞，遥相关，SST 异常，风暴路径